Experimental Characterization of the High Frequency Response of the LHO 4k IFO

C: Test Mass Resonances, Up-Converted Noise and Transverse Modes

LIGO-T040003-00-D

W.E. Butler and A.C. Melissinos
Department of Physics & Astronomy,
University of Rochester, Rochester NY. 14627

January 12, 2004

As part of the characterization of the high frequency response of the Hanford 4K interferometer [1, 2] we observed and analyzed two internal test mass resonances in the vicinity of $f \simeq 38$ kHz. We also observed the up-conversion of the low frequency seismic and suspension noise. Finally we discuss the observation of the transverse modes of the X-arm cavity. This was achieved by sideband injection; the deduced curvature of the test-mass mirrors is in reasonable agreement with the design value.

1 Test Mass Internal Resonances

The test masses are subject to elastic oscillations due to the finite temperature of the environment, what is referred to as Brownian motion. Such oscillations induce a phase shift on the incident (and stored) laser beam and thus contribute a "random" noise at the readout channel, in particular at low frequencies. The motion of the mirror surfaces can be expanded in the normal modes (resonances) of the test mass, as detailed by Gillespie and Raab [3, 4]. The individual mode n contributes to the displacement power density at the frequency $f = \omega/(2\pi)$.

$$S_{xn}(f) = \frac{4k_BT}{\alpha_n m\omega}\left[\frac{\omega_n^2\phi_n(\omega)}{(\omega^2-\omega_n^2)^2+\omega_n^4\phi_n^2(\omega)}\right] \tag{1}$$

where k_B, T are the Boltzmann constant and temperature; ω_n is the resonant angular frequency of the mode, m the mass of the optic and $\omega = 2\pi f$; α_n is an effective mass coefficient which accounts for the coupling of that particular mode to the laser beam. The coefficient α_n can vary between $10^{-2}-10^{1}$. $\phi_n(\omega)$ is the loss function, and on resonance, $\phi_n(\omega_n) = 1/Q_n$ where Q_n is the quality factor of the mode.

At frequencies much lower than ω_n, one can sum all the modes to find the total displacement power density [3, 4].

$$S_x(f) \simeq \sum_n \frac{4k_BT}{\alpha_n m\omega_n^2}\,\frac{\phi_n(\omega)}{\omega} \quad \left(\frac{\mathrm{m}^2}{\mathrm{Hz}}\right) \tag{2}$$

Simulations by Gillespie and Raab find that for $f = 100$ Hz the LIGO 4km IFO has

$$S_x(100\text{ Hz}) \simeq 8\times 10^{-40}\mathrm{m}^2/\mathrm{Hz}$$

Similar results were obtained by Y. Levin [5] using a more general technique.

Fig.1 shows the response of the full IFO to a frequency sweep of ITMX. The same data was presented in our previous report where parametric conversion was discussed [2]. In that case however the data was cropped at 37.7 kHz to exclude the two peaks appearing at 37.804 and 37.971 kHz. We attribute these peaks to internal resonances (modes) of the optic driven by the exciting force applied to the back plane.

To fit the data we model the test mass as a simple harmonic oscillator [3, 4] in which case the force to displacement transfer function is [6]

$$H(f) = \frac{1}{[1-(\omega/\omega_n)^2 + i(\omega/\omega_n)\phi_n(\omega)]} \tag{3}$$

Replacing $\phi_n(\omega)$ by $1/Q$ and introducing a normalization factor N/Q, we write for the measured transfer function (Volts drive to Volts signal)

$$H(f) = \frac{N/Q}{1-(\omega/\omega_n)^2 + (i/Q)(\omega/\omega_n)} \tag{4}$$

On resonance $|H(f_n)| = N$ independently of the Q-value.

While Eq.(4) is suitable for fitting the data, the real Q-value cannot be extracted because of the frequency resolution with which the data was acquired. Typically we expect $Q \sim 10^6$ to 10^7 which implies a full width of .04 to .004 Hz as compared to the resolution of the data $\Delta f = 1$ Hz. Thus the values of Q returned by the fit are lower limits of the real Q_n.

The two resonance peaks were first fit independently to Eq.(4) in order to determine the corresponding values of N and $Q_{\text{min.}}$. Then the two resonances were combined with the parametric conversion response of the IFO [2] to produce an overall fit in the range 37.3 to 38.0 kHz. In this case each of the internal resonances was given an adjustable phase and a noise floor was added as well. The results of the fits are shown in Tables 1 and 2.

Table 1: Test Mass Internal Resonances

Central Frequency f (Hz)	Q_{min}	Normalization N
37804.5 ± 0.5	1.03×10^5	1.87×10^{-4}
37971.7 ± 0.5	1.00×10^4	5.65×10^{-6}

Table 2: Overall Fit Parameters

Resonance #1	Phase	-171^o
Resonance #2	Phase	1^o
Noise Floor	Phase	174^o
Noise Floor	Magnitude	3.4×10^{-7}
Overall Additive	Phase	93^o

As can be seen in Fig. 1 these parameters produce an excellent fit not only to the magnitude of the response but also to the measured phase over the entire frequency band.

Since we are interested in a possible stochastic signal at 37.52 kHz we need to know the contribution from the internal resonances (thermal noise) and in particular from the adjacent resonances analyzed above. For the resonances, lying well above 37.52 kHz we can use Eq.(2) and scale the corresponding numerical result from $f = 100$ Hz to 37.52 kHz. We obtain

$$S_x(37.52 \text{ kHz}) = \frac{100}{37.52 \times 10^3}\, S_x(100 \text{ Hz}) = 2.1 \times 10^{-42} \quad \frac{\text{m}^2}{\text{Hz}}$$

The rms displacement density is the square root of S_x so that

$$h = \frac{x}{L} = \frac{\sqrt{S_x}}{L} = 3.7 \times 10^{-25}/\sqrt{\text{Hz}} \tag{5}$$

To evaluate the contribution of the two nearest resonances, $f_n = 37.804$ kHz and 37.972 kHz we must use Eq.(1) and sum the two contributions. However $\phi_n(\omega)$ and α_n are not known. If we use the accepted values of $\phi_n = 10^{-7}$ and $\alpha_n = 0.5$, as well as $m = 12.2$ kg we obtain

$$S_{xn}(37.52 \text{ kHz}) = 1.3 \times 10^{-40} \quad \text{m}^2/\text{Hz}$$

whereas if we use $\phi_n = 1/Q_{\min}$ as obtained from the fit

$$S_{xn}(37.52 \text{ kHz}) < 4.5 \times 10^{-38} \quad \text{m}^2/\text{Hz}$$

and correspondingly the strain sensitivity is

$$\begin{aligned} h = \frac{x}{L} = \frac{\sqrt{S_x}}{L} &= \ 2.8 \times 10^{-24}/\sqrt{\text{Hz}} \\ h = \frac{x}{L} = \frac{\sqrt{S_x}}{L} &< \ 5.3 \times 10^{-23}/\sqrt{\text{Hz}} \end{aligned} \tag{6}$$

for $\phi_n = 10^{-7}$ and $\phi_n = 1/Q_{\min}$ respectively. This result is an order of magnitude higher than the contribution given by Eq.(5).

From the calibration of the ITMX motion [2] we had found that $\Delta x = 8 \times 10^{-16}$ m at 37.52 kHz generates a signal of $V_s = 87 \times 10^{-6}$ V. The noise floor for a bandwidth $B = 0.0625$ Hz as shown in Fig. 4 is at $V_n = 40 \times 10^{-9}$ V. Consequently the sensitivity that can be obtained from a single FFT at that bandwidth is

$$h_s = \frac{x}{L} = \frac{1}{L}\frac{\Delta_x}{V_s}\frac{V_n}{\sqrt{B}} = 3.7 \times 10^{-22}/\sqrt{\text{Hz}}$$

This calibration is for a single arm; a gravitational wave will produce a differential signal in both arms, thus the same signal would indicate half the strain. In 24 hours of data taking 86,400 measurements with a 1 Hz bandwidth can be acquired. When they are averaged the fluctuations should be reduced by a factor of 294, so that the fluctuations are

$$\Delta h_s \simeq 6 \times 10^{-25} \tag{7}$$

which is less than the thermal noise predicted by Eq.(6).

2 Up-converted Seismic and Suspension Noise

FFT's obtained with high resolution when the test mass was driven at the fixed frequency of 37.52 kHz are shown in Figs. 2, 3 and 4. As expected they show a strong response at the

driving frequency since it corresponds to the fsr (free spectral range) of the IFO. However the FFT's also exhibit sidebands around the main peak. The symmetric appearance of the sidebands indicates that they are due to low frequency oscillations up-converted to near the driving frequency.

If the amplitude of the low frequency oscillation (at f_β) is x_β then the sidebands will appear at frequencies $(f_0 \pm f_\beta)$ and with a relative amplitude $A_\beta/A_0 = 2kx_\beta$. Here f_0 is the driving frequency and A_0 the amplitude of the response at f_0; k is the wavenumber of the laser light $k = 2\pi/\lambda$. We have assumed that the low frequency oscillations are independent of the high frequency excitation and that the mixing occurs at the detection of the light; recall that the diode signal is proportional to $|E_{\rm total}|^2$.

While all three FFT's exhibit low frequency sidebands the details of the spectrum differ. The data in Figs. 2 and 3 were taken in December 2002; Fig. 2 with a 0.5 V drive 0.125 Hz bandwidth and 483 averages. Fig. 3 with a 1 V drive, 0.0625 Hz bandwidth and 41 averages. The data in Fig. 4 were obtained in October 2002 and correspond to different operating conditions of the IFO; the drive was 2 V, the bandwidth 0.0625 Hz and only 11 averages were taken. The discrete lines at a fraction of a Hz and at a few Hz are identified as oscillation modes of the suspension, while the broader features, especially apparent in Fig. 3, are attributed to seismic noise.

To provide some quantitative measure of these data we have fitted the spectra as follows: A Gaussian was used for the central peak since it's width is instrumental, and each sideband was fit by a Lorentzian [Eq.(4)]. In addition a noise floor was included. In Fig. 3 the central peak was fitted by a double Gaussian in order to account for some of the low frequency seismic noise. The quality of the fits can be judged better by the log-log plots shown in Figs. 2B, 3B and 4B. The results of the fits are summarized in Table 3 where we give the sideband offset frequency and relative amplitude separately for each of the three spectra.

The peak at $\sim$0.75 Hz is clearly the pendulum mode of the suspension which is known to be at 0.71 Hz [7]. The peak around 2 Hz may be the third harmonic of the above resonance; possibly the peak at 1.3 Hz seen in Fig. 4 could be the second harmonic. The prominent peaks in Fig. 4 at $\sim$11 Hz and $\sim$19 Hz can be identified with the bounce mode of the suspension which is located at 11.9 Hz and the roll mode, expected to be at 17.5 Hz [7]. If we use an average value of the relative amplitude as $A/A_0 \simeq 10^{-2}$ we conclude that $x_\beta \simeq 8 \times 10^{-10}$ m which is of the order of the thermal excitation of such low frequency modes [using Eq.(1) and $Q \simeq 10^4$].

Finally we consider the quasi-continuous noise level extending out to $\sim$15 Hz and that is most pronounced in Fig. 3. We believe that it is due to seismic noise exciting the mirror suspension as well as tables and chambers on which the optics are mounted. Support for this interpretation is provided by Fig. 5 which shows low frequency measurements made with a seismometer (top) in the LVEA and of the motion of the Beam Splitter, ITMX and ITMY (bottom). The similarity of this spectrum with the sidebands in Fig. 3 is notable, including the cut-off at $\sim$15 Hz which is probably due to vibration suppression or active feedback.

Table 3: Up-converted Noise

	From fig.2	From fig.3	From fig.4
f_1(Hz)	0.75	0.73	0.61
A_1/A_0	7×10^{-3}	7.9×10^{-3}	1.6×10^{-2}
f_2(Hz)	$--$	$--$	1.35
A_2/A_0	$--$	$--$	1.3×10^{-2}
f_3(Hz)	1.91	2.09	2.01
A_3/A_0	7×10^{-3}	8.3×10^{-3}	7×10^{-3}
f_4(Hz)	7.60	$--$	$--$
A_4/A_0	10^{-3}	$--$	$--$
f_5(Hz)	$--$	$--$	11.90
A_5/A_0	$--$	$--$	3.8×10^{-2}
f_6(Hz)	$--$	$--$	17.44
A_6/A_0	$--$	$--$	2×10^{-2}
f_7(Hz)	$--$	$--$	19.13
A_7/A_0	$--$	$--$	2.3×10^{-2}

3 Transverse Modes

It is well known that optical cavities will support Hermite-Gaussian modes of the fields [8, 9]. Such modes are distinguished by the axial index $n \simeq L/2\lambda$ (L is the length of the cavity and λ the wavelength) and labeled by the small integers m, ℓ which specify the field distribution in the two directions transverse to the cavity axis. For a cavity with spherical mirrors of radii R_1 and R_2 the frequency of the n, m, ℓ mode is

$$\nu_{nm\ell} = \frac{c}{2L}\left[n + (1 + m + \ell)\frac{\cos^{-1}\sqrt{g_1 g_2}}{\pi}\right] \tag{8}$$

and

$$g_i = 1 - L/R_i \qquad\qquad i = 1, 2 \tag{9}$$

We decided to search for the lowest transverse mode [10] by injecting a sideband onto the carrier. When the sideband frequency is exactly at the difference between the populated

TEM_{00} mode and a transverse mode, a dip should be observed in the demodulated signal as demonstrated in the case of the fsr [1].

The IFO is injected with a laser beam precisely aligned to the axis of the optical cavity and matched to the TEM_{00} mode. Thus the transverse modes are not excited in the arm. To observe the transverse mode we locked a single arm and intentionally misaligned the cavity. Using the digital suspension controls, the input test mass was rotated either around a vertical axis (yaw) or a horizontal axis (pitch). This coupled the input laser beam to the $\ell = 1, m = 0$ (horizontal) mode in the first case or to the $\ell = 0, m = 1$ (vertical) mode in the second. Fig. 6 shows a typical response curve obtained when the suspension control "slider" was set at 2.241 units; the observed frequency was 11.48 kHz.

Misalignment of the ITM not only increases the coupling to the transverse mode but also shifts the frequency of the mode. This was immediately evident from the data shown in Fig. 7 for the horizontal mode and in Fig. 8 for the vertical mode. In these figures the mode frequency is shown as a function of pitch or yaw of the ITM, the angle being labeled in slider units. Since the frequency shift must be symmetric with respect to the pitch or yaw angle the lowest contribution is proportional to the angle squared. Therefore a quadratic fit was made to the data as shown. The peak of the curve corresponds to the properly aligned cavity for which the measured frequency shifts are

$$\begin{aligned} \Delta\nu_{\text{horizontal}} &= 11,530 \pm 5 \text{ Hz} \\ \Delta\nu_{\text{vertical}} &= 11,560 \pm 5 \text{ Hz} \end{aligned} \tag{10}$$

From Eq.(9) we see that the frequency shift is related to the mirror curvatures by

$$\Delta\nu = \frac{\nu_{\text{fsr}}}{\pi} \cos^{-1}(\sqrt{g_1 g_2}) \tag{11}$$

and find

$$\begin{aligned} g_1 g_2 &= 0.3239 \pm 0.0004 \qquad \text{horizontal mode} \\ &= 0.3215 \pm 0.0004 \qquad \text{vertical mode} \end{aligned}$$

The values deduced from the measurement of the two modes differ by $\sim 4\sigma$ and this may be due to a deformation of the mirror surface.

The design values for the curvature are given in [11] and the "as built" values [12] are

$$\begin{aligned} R_1 &= 14,240 \text{ m} \qquad \text{(ITM)} \\ R_2 &= 7,260 \text{ m} \qquad \text{(ETM)} \end{aligned}$$

This leads to

$$g_1 = 0.719 \qquad g_2 = 0.450 \qquad \text{and} \qquad g_1 g_2 = 0.324$$

in close agreement with the $g_1 g_2$ product obtained from the frequency of the horizontal mode.

References

[1] William E. Butler and Adrian C. Melissinos. Experimental Characterization of the High Frequency Response of the LHO 4k IFO, A: Sideband Injection. Technical report, University of Rochester, Dept. of Physics & Astronomy, 2003. LIGO Internal #: T030163.

[2] William E. Butler and Adrian C. Melissinos. Experimental Characterization of the High Frequency Response of the LHO 4k IFO, B: Parametric Conversion. Technical report, University of Rochester, Dept. of Physics & Astronomy, 2003. LIGO Internal #: T030263.

[3] A. Gillespie and F. Raab. Thermally excited vibrations of the mirrors of LASER interferometer gravitational-wave detectors. *Physical Review D*, 52(2):577–585, July 1995.

[4] Peter R. Saulson. Thermal noise in mechanical experiments. *Physical Review D*, 42(8):2437–45, October 1990.

[5] Yu. Levin. Internal thermal noise in the LIGO test masses: A direct approach. *Physical Review D*, 57(2):659–663, January 1998.

[6] Leonard Meirovitch. *Elements of Vibration Analysis*. McGraw-Hill Book Company, 1975.

[7] Michael Landry and David Ottaway. Summary of mechanical resonances in the LIGO Hanford interferometers. Technical report, LIGO Internal #: T000020, March 2000.

[8] Anthony E. Siegman. *LASERS*. University Science Books, 55D Gate Five Road Sausalito, California 94965, 1986.

[9] Frank L. Pedrotti and Leno S. Pedrotti. *Introduction to Optics*. Prentice Hall, Upper Saddle River, New Jersey 07458, 1993.

[10] W. Butler, A. Melissinos, and F. Raab. Experimental determination of the mode spectrum of the locked arms of the Hanford 4k Interferometer". Internal note July 3, 2002. The same suggestion was made independently by F. Bondu and R. Savage: private communication.

[11] G. Billingsley, B. Kells, H. Yamamoto, J. Camp, D. Li, H. Armandula, S. Bell, and S. Elieson. Core optics components final design. Technical report, Caltech, April 1998. LIGO Internal #: E980061.

[12] GariLynn Billingsley. COC as built. LIGO Internal Web page.

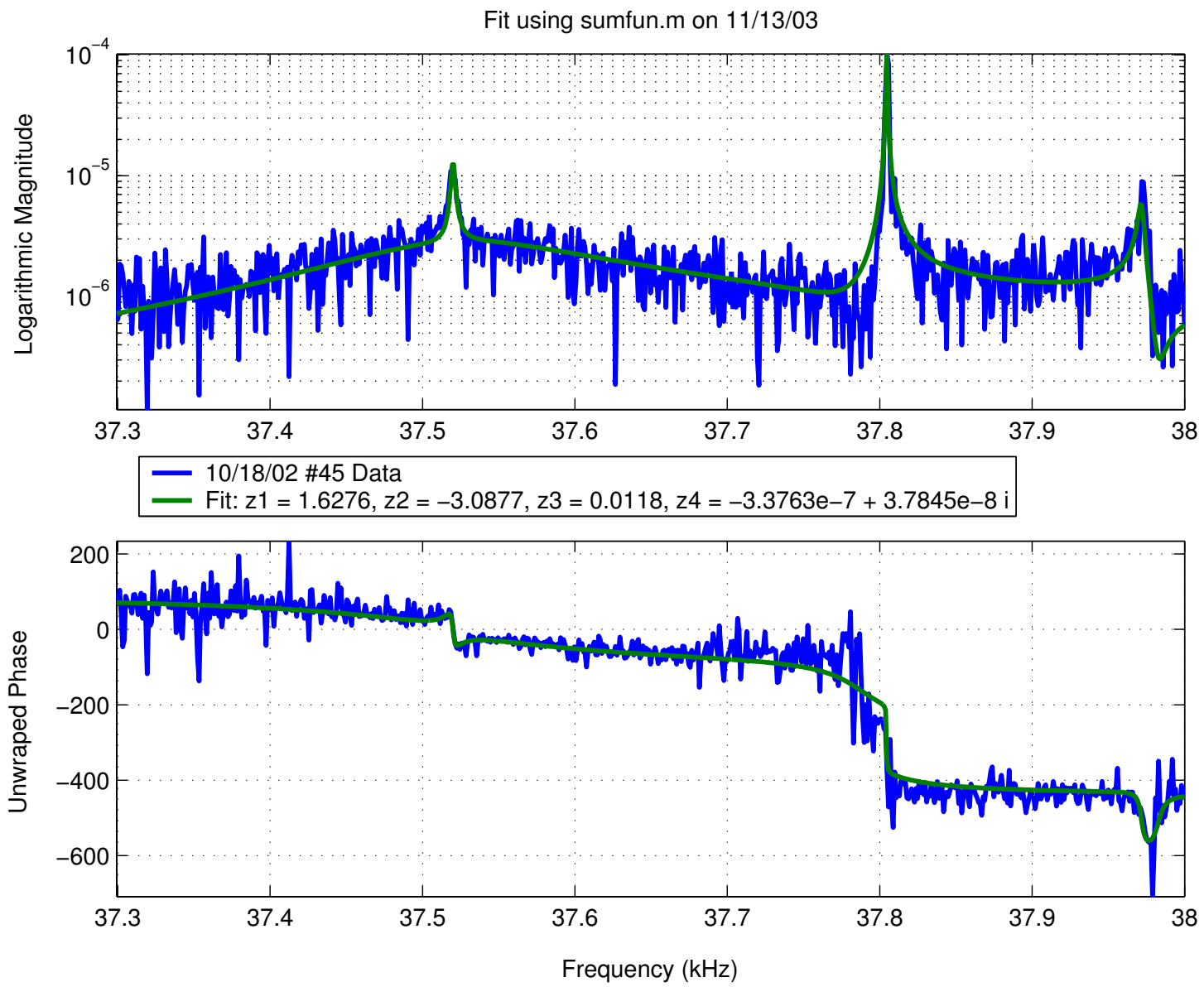

Figure 1: Swept Sine Response to ITM excitation in full PRIFO configuration.

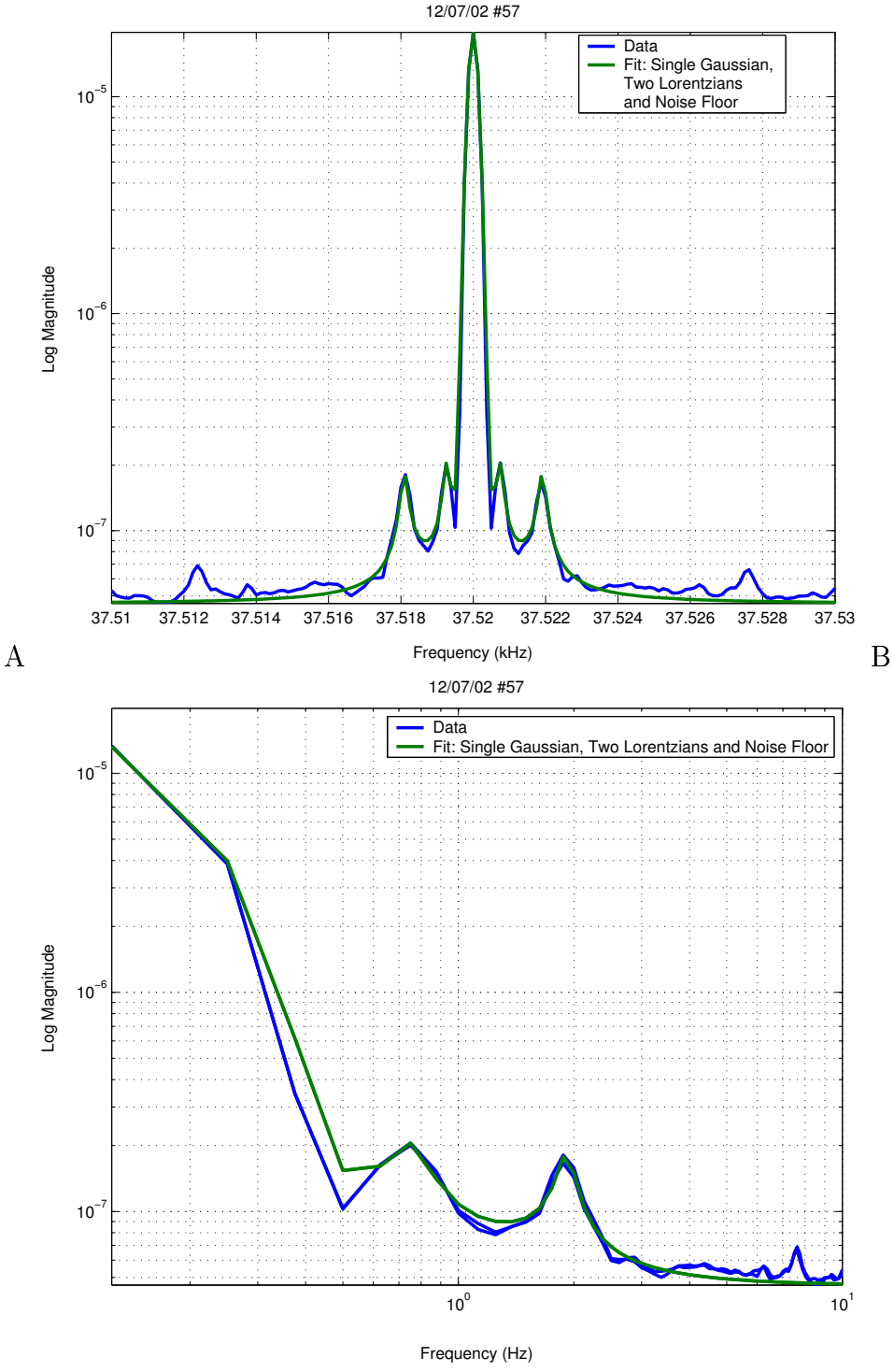

Figure 2: FFT of AS_I with mass excitation of $0.5V_{pk}$ @ 37.52 kHz taken in December of 2002. Linear frequency and Log frequency plotted as magnitude frequency away from 37.52 kHz

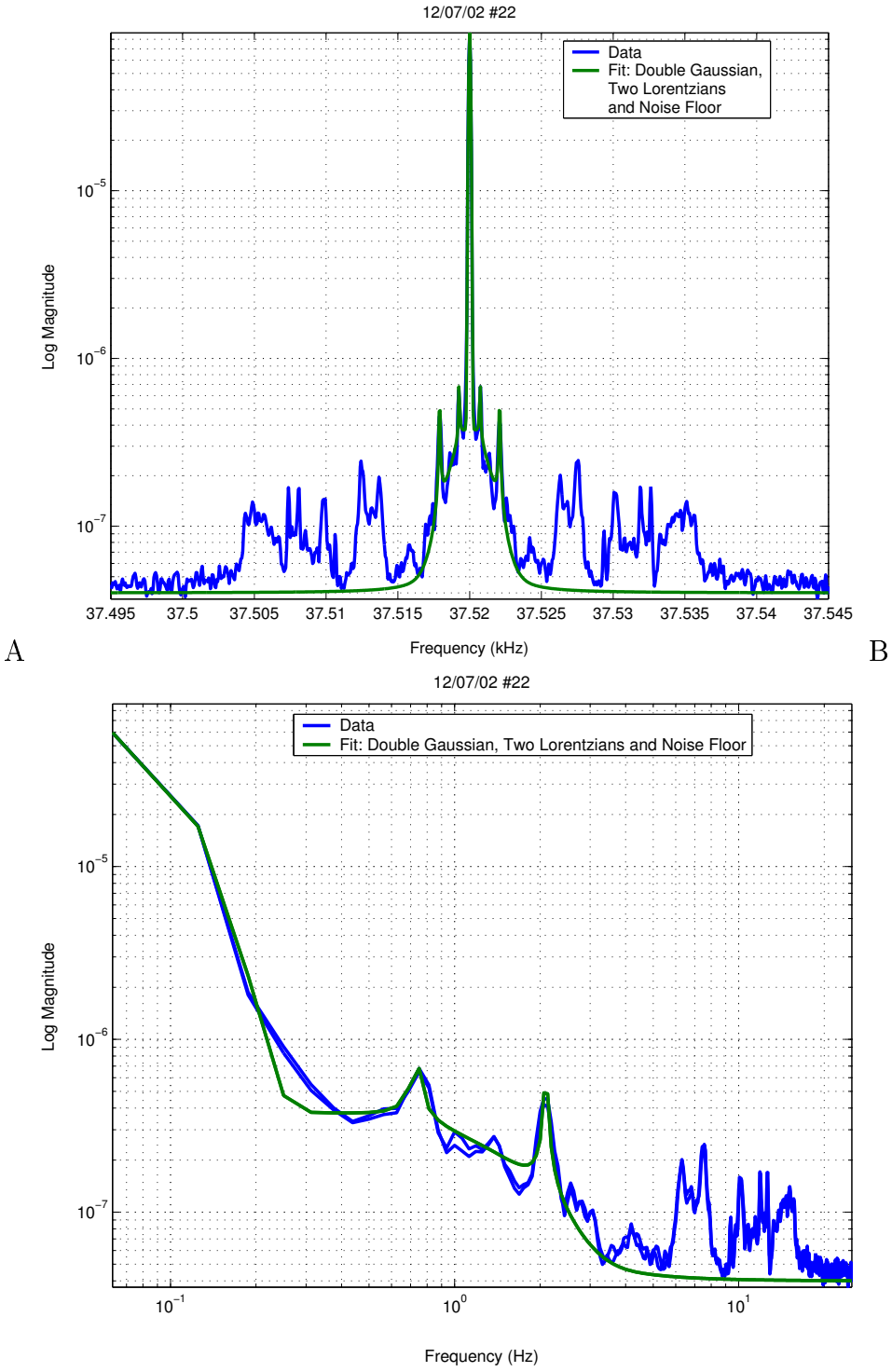

Figure 3: FFT of AS_I with mass excitation of $1.0V_{pk}$ @ 37.52 kHz taken in December of 2002. Linear frequency and Log frequency plotted as magnitude frequency away from 37.52 kHz

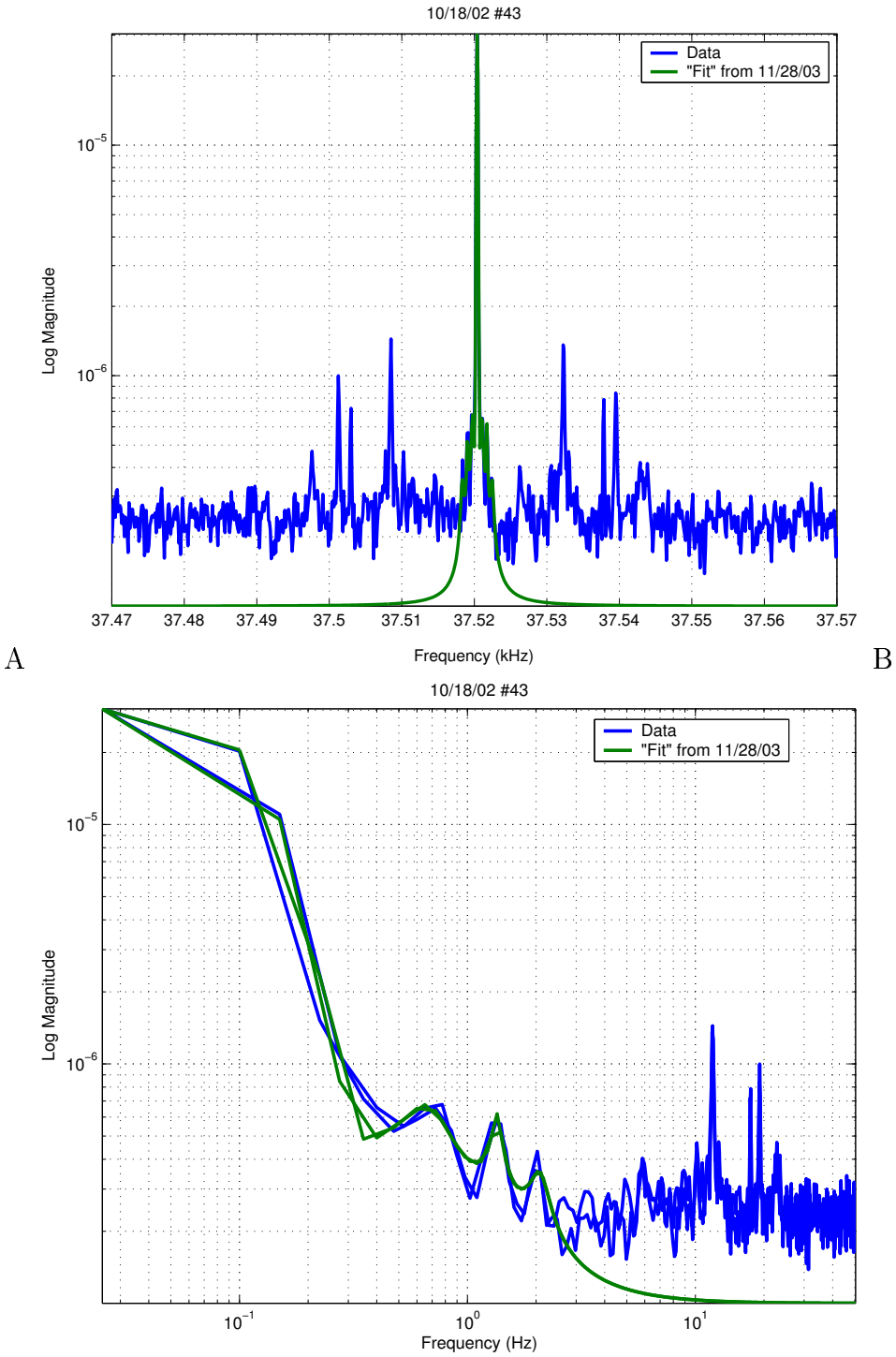

Figure 4: FFT of AS_I with a 2V excitation @ 37.52 kHz taken in October of 2002 (at this time the drive was not calibrated). Linear frequency and Log frequency plotted as magnitude frequency away from 37.52 kHz

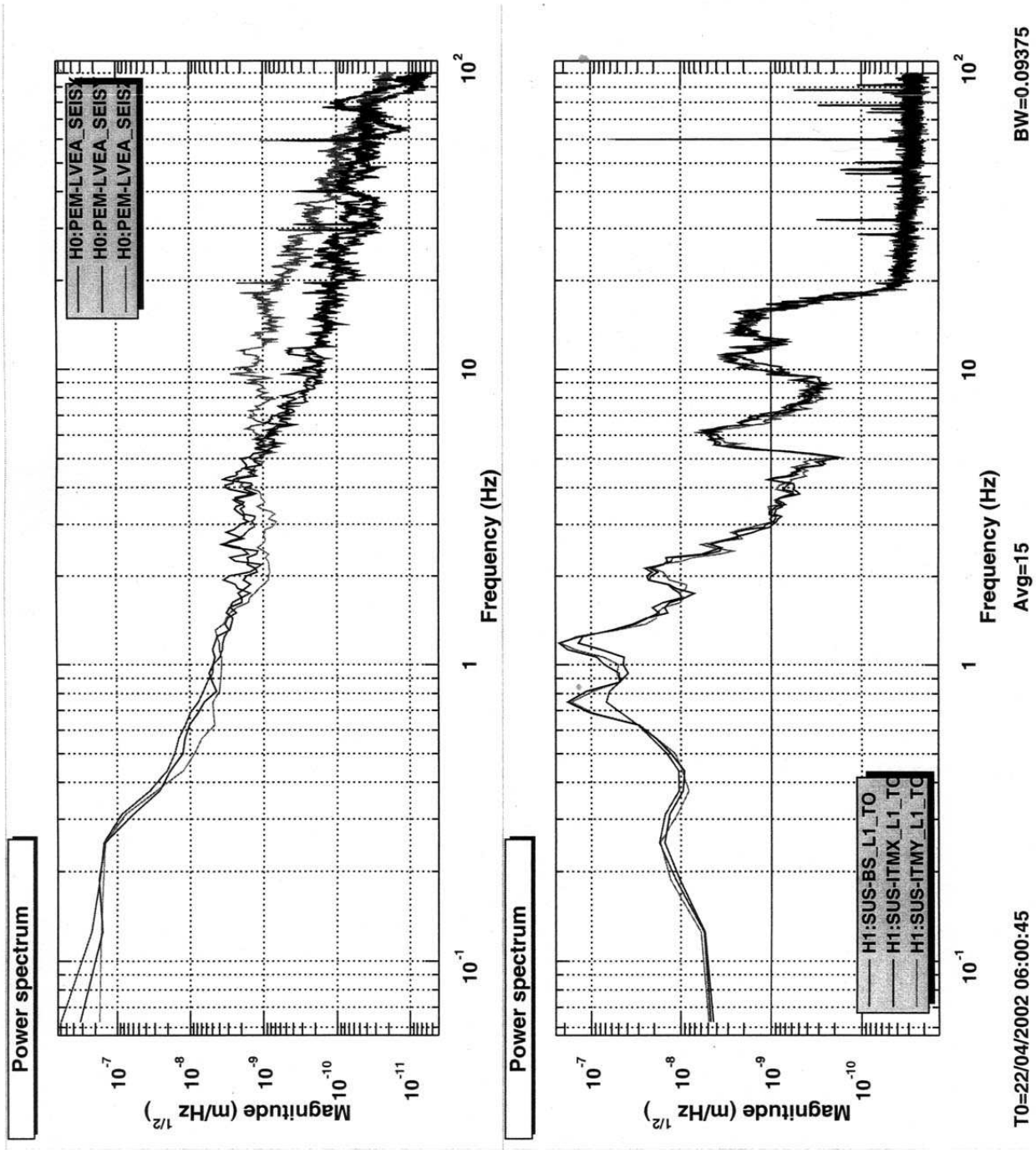

Figure 5: Seismic Noise Spectrum

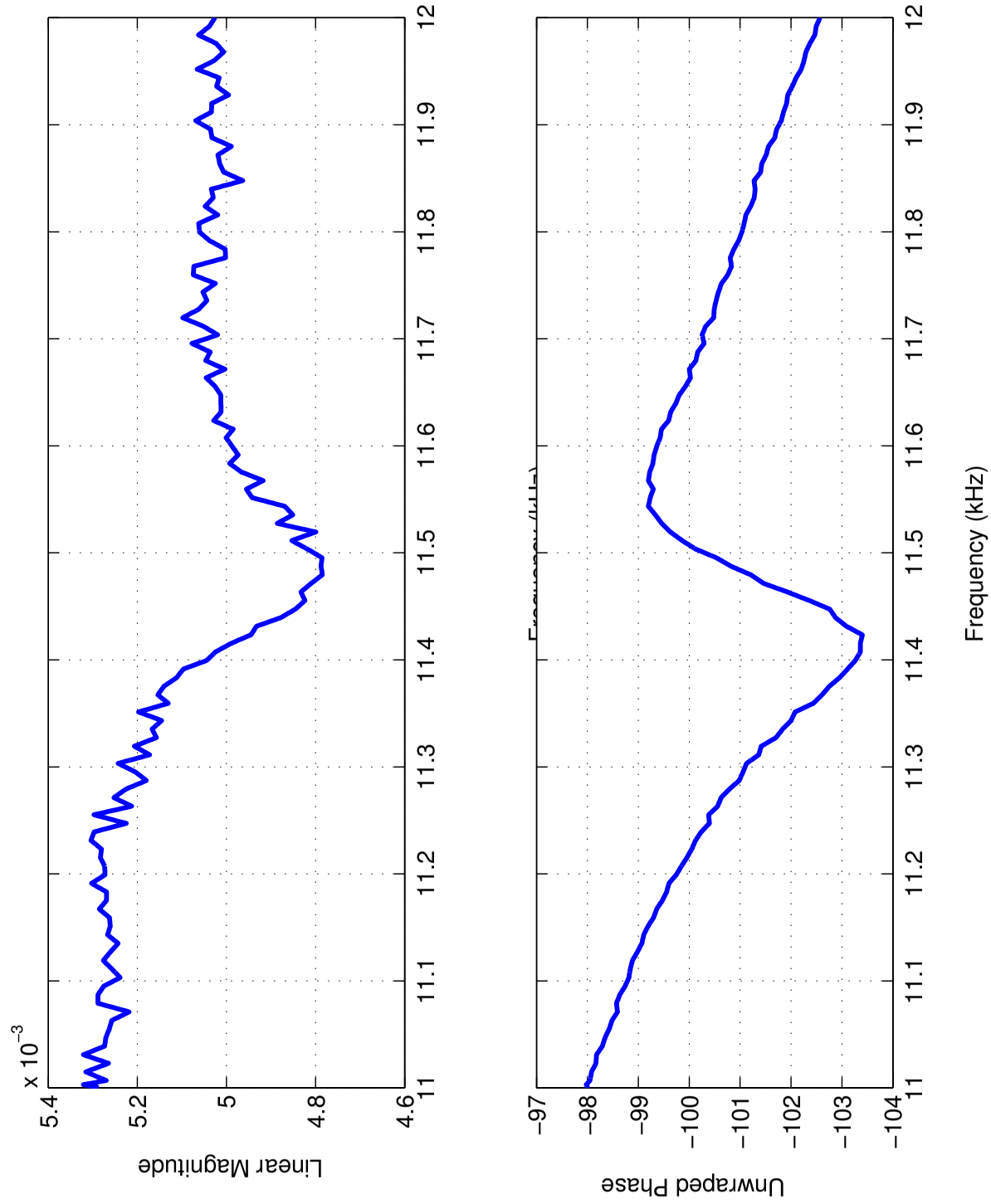

Figure 6: Sideband Injection Sweep for Transverse Mode Characterization

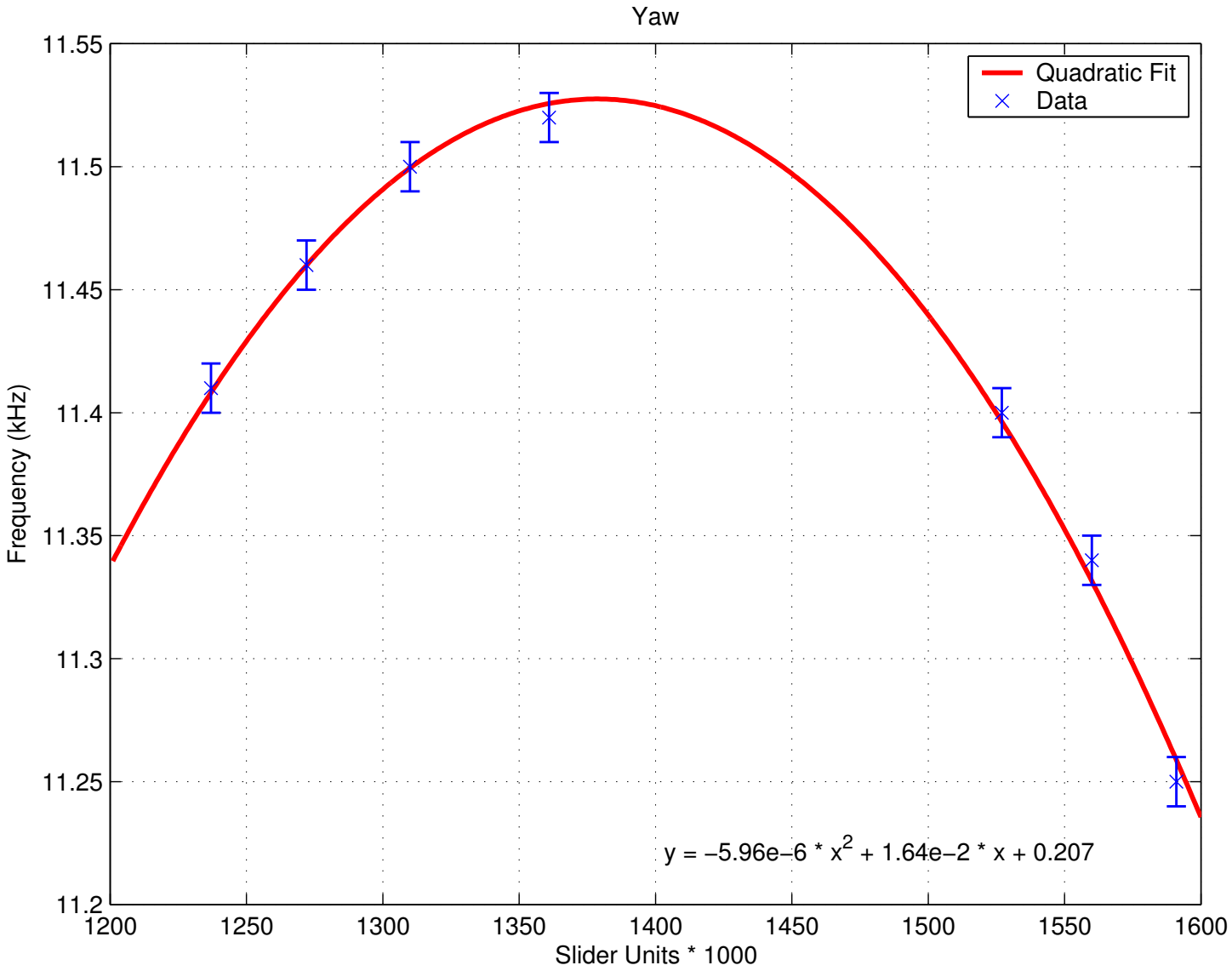

Figure 7: Transverse Mode Frequency variance with Yaw

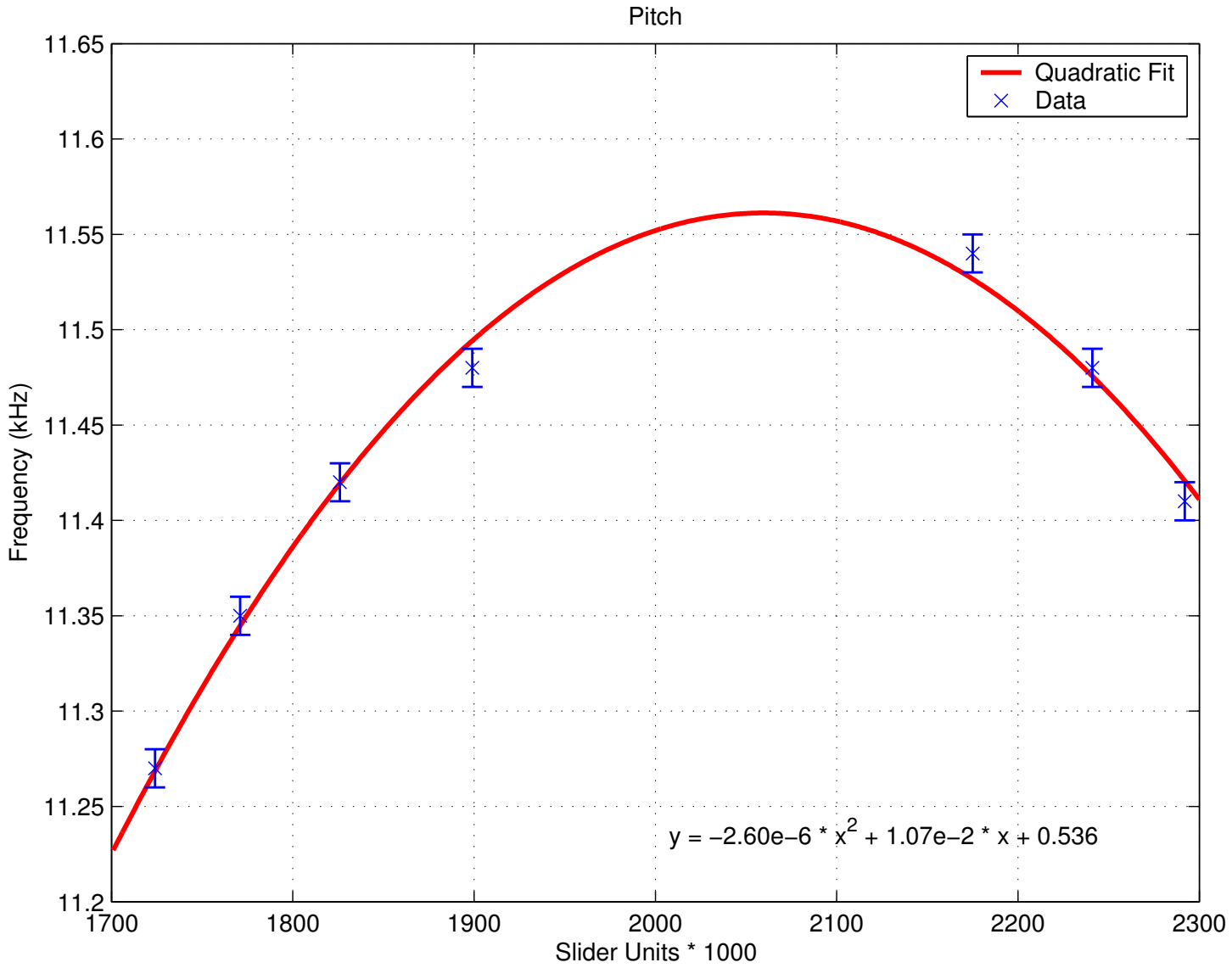

Figure 8: Transverse Mode Frequency variance with Pitch